Proceedings IRF2018: 6th International Conference Integrity-Reliability-Failure
Lisbon/Portugal 22-26 July 2018. Editors J.F. Silva Gomes and S.A. Meguid
Publ. INEGI/FEUP (2018); ISBN: 978-989-20-8313-1

PAPER REF: 7085

THE EFFECTS OF SOIL CATEGORY ON THE SEISMIC RESPONSE OF CIRCULAR STEEL WATER TANKS WITH MEDIUM H/D RATIO USING LAGRANGIAN APPROACH

Armen Assatourians[1(*)], Sohrab Fallahi[2]

[1]Earthquake Engineering Research Consultant, Yerevan Project Co., Yerevan, Armenia
[2]Senior Structural Designer, E.S.S. Consulting Eng. Co., Tehran, Iran
[(*)]*Email:* ar_ast@mail.ru

ABSTRACT

Water Tanks are amongst the most important special structures which are used for storage and providing the needed water on the pick usage time in water supply networks. According to this, investigating the seismic behavior of these structures are of much importance. In current research, the seismic response of cylindrical steel water tanks with medium H/D ratio, by the means of Lagrangian approach for considering the fluid-structure interaction, is studied. Analysis procedure of the whole water-tank system is completed by the means of Time History Analysis method, using 5 pairs of horizontal components of selected accelerograms, recorded on soil categories of Rock, Dense Soil, Loose Soil and Very Loose Soil and scaled to spectral acceleration level of S_a=0.35g. The response is computed for the filling strategy of Empty, 50% Full and 100% Full conditions of both shapes and the final results are summarized and discussed.

Keywords: Time History Analysis, Round Steel Water Tanks, Spectral Acceleration, Soil Category, Lagrangian Approach

INTRODUCTION

The on grade cylindrical tanks are the type of lifeline structures which are extensively used in water supply facilities, oil and gas refineries and nuclear power plants for various purposes. Extensive failures and damages observed in the on-grade cylindrical steel tanks have persuaded the researchers to investigate the seismic behaviour of these special structures. Housner (1963), in a pioneering work, divided the hydrodynamic response of a rigid tank into two liquid impulsive and convective masses. The part of the liquid that vibrates with the tank's rigid body produces the impulsive mode of response, while the rest of the liquid generates the sloshing mode and is identified with a long period of vibration.

LAGRANGIAN APPROACH THEORY

Basic formulation for fluid-structure interaction using finite element method with Lagrangian approach is summarized below:

1) Fluid is compressible and linear static. The used finite element is based on a formulation in which the fluid strains are calculated from the linear strain-displacement equations. The only strain energy considered is associated with the compressibility of the fluid (Wilson and Khalvati, 1983). The pressure volume relationship for linear fluid is given by equation (1).

$$p=E_v\ \varepsilon_v\ , \tag{1}$$

where the pressure p is equal to the magnitude of the mean stress, E_y is the bulk modulus of fluid and ε_v is the volumetric strain.

2) Viscosity effects are negligible. This assumption is not contrary to the fact since the effect of viscosity for the dynamic behavior of fluid storage tanks is negligible and this effect decreases when the dimensions of the tanks increase (Priestley 1986).

3) Displacement field is considered to be irrotational by introduction of a rotational stiffness. If the fluid is assumed to have no shear strength, and the elasticity matrix for the fluid is with the shear modulus set to zero. This results in a singular stress-strain matrix which in turn leads to spurious, zero-energy deformation modes for fluid elements and fluid meshes. A possible method of overcoming this problem is to assume a small value for shear modulus of the fluid. A second approach is to admit the inviscid behavior and to use the implication that the fluid must be irrotational in nature. This behavior can be enforced by the use of a penalty function as used in this study. Rotations (ε_{xr}, ε_{yr}, ε_{zr}) and constraint parameter (E_{11}, E_{22}, E_{33}, E_{44}) for the x, y and z directions, which are necessary to satisfy the rotation constraints in this assumptions, are as equation (2).

$$\varepsilon_{xr} = \frac{1}{2}\left[\frac{\partial u_z}{\partial y} - \frac{\partial u_y}{\partial z}\right] \qquad \varepsilon_{yr} = \frac{1}{2}\left[\frac{\partial u_x}{\partial z} - \frac{\partial u_z}{\partial x}\right] \qquad \varepsilon_{zr} = \frac{1}{2}\left[\frac{\partial u_y}{\partial x} - \frac{\partial u_x}{\partial y}\right] \tag{2}$$

$$E_{11} = E_v \qquad E_{22} = \psi_x E_v \qquad E_{33} = \psi_y E_v \qquad E_{44} = \psi_z E_v \tag{3}$$

where $\boldsymbol{\psi_x}$, $\boldsymbol{\psi_y}$ and $\boldsymbol{\psi_z}$ are constraints parameter coefficients. From here, rotation pressures (p_{xr}, p_{yr}, p_{zr}) are as equation (4).

$$p_{xr} = E_{22}\varepsilon_{xr} \qquad p_{yr} = E_{33}\varepsilon_{yr} \qquad p_{zr} = E_{44}\varepsilon_{zr} \tag{4}$$

The total potential energy (U) of the fluid system consist of the sum of the strain energy (Π_ε) and the increase in potential energy (Π_s) by taking into account the free surface oscillations of the fluid. The expression for this energy is as equation (5).

$$U = \Pi_\varepsilon + \Pi_s \rightarrow U = \frac{1}{2}\int \varepsilon^T E \varepsilon dV + \frac{1}{2}\int u_s \rho g(H + u_s)dv \tag{5}$$

Where E is elasticity matrix, us is the vertical displacement of the fluid, H is the height of the fluid, g is the acceleration due to gravity and ρ is the mass density of fluid. The kinetic energy (T) of the fluid is according to equation (6).

$$T = \frac{1}{2}\int \rho v^T v dv \tag{6}$$

where $v(v^T=[v_x \;\; v_y \;\; v_z])$ is the velocity vector in the Cartesian coordinates. Three dimensional isoperimetric fluid element with eight nodes is considered in Lagrangian approach. Global (*x, y, z*) and local axes (*r, s, t*) are given in Figure 1 for this element.

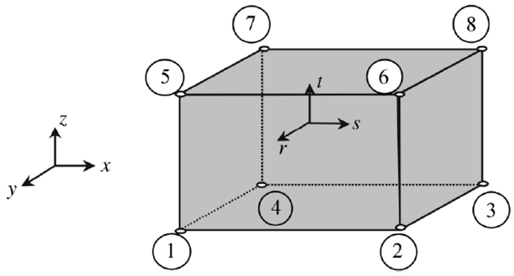

Fig. 1 - 8 node fluid finite element

Expressions for mass and rigidity matrices are given in equations (7) and (8).

$$\boldsymbol{M} = \rho\int_v \boldsymbol{Q}^T\boldsymbol{Q}dV \rightarrow \boldsymbol{M} = \rho\sum_i\sum_i\sum_k \boldsymbol{\eta}_i\boldsymbol{\eta}_j\boldsymbol{\eta}_k\boldsymbol{Q}^T_{ijk}\boldsymbol{Q}_{ijk}\det\boldsymbol{J}_{ijk} \tag{7}$$

$$\boldsymbol{K} = \int_v \boldsymbol{B}^T\boldsymbol{E}\boldsymbol{B}dV \rightarrow \boldsymbol{K} = \sum_i\sum_j\sum_k \boldsymbol{\eta}_i\boldsymbol{\eta}_j\boldsymbol{\eta}_k\boldsymbol{B}^T_{ijk}\boldsymbol{E}\boldsymbol{B}_{ijk}\det\boldsymbol{J}_{ijk} \tag{8}$$

where $\boldsymbol{J}$ is the Jacobian matrix, $\boldsymbol{Q}_{\mathrm{ijk}}$ is the interpolation function, η_i, η_j and η_k are weighting functions, $\boldsymbol{B}$ is the strain-displacement function obtained from $\boldsymbol{\varepsilon} = \boldsymbol{B}\; u$ expression. Rigidity occurred from oscillation on the surface.

$$\boldsymbol{S} = \rho g\int_A \boldsymbol{Q}_s^T\boldsymbol{Q}_s dA \rightarrow \boldsymbol{S} = \sum_i\sum_j \boldsymbol{\eta}_i\boldsymbol{\eta}_j\boldsymbol{Q}^T_{sij}\boldsymbol{Q}_{sij}\det\boldsymbol{J}_{ij} \tag{9}$$

where Q_s is the interpolation function for two dimensional surface element. After the mass and rigidity functions are obtained from equations (7) and (8), total potential and kinetic energy expressions in the finite element can be written as equations (10) and (11) respectively:

$$U = \Pi_\varepsilon + \Pi_s \rightarrow U = \frac{1}{2}\boldsymbol{u}^T\boldsymbol{K}\boldsymbol{u} + \frac{1}{2}\boldsymbol{u}_s^T\boldsymbol{S}\boldsymbol{u}_s \tag{10}$$

$$T = \frac{1}{2}\boldsymbol{v}^T\boldsymbol{M}\boldsymbol{v} \tag{11}$$

If the potential and kinetic energy expressions are substituted in the Lagrangian equation (12).

$$\frac{d}{dt}\left(\frac{\partial T}{\partial \dot{u}_j}\right) - \frac{\partial T}{\partial u_j} + \frac{\partial u}{\partial u_j} = F_j \tag{12}$$

where u_j is the j^{th} displacement component and F_j is the applied external load, the governing equation can be written as equation (13).

$$\boldsymbol{M}\ddot{\boldsymbol{u}} + \boldsymbol{K}\boldsymbol{u} + \boldsymbol{S}\boldsymbol{u}_s = \boldsymbol{R} \tag{13}$$

where $\ddot{u}$ is the acceleration and $\boldsymbol{R}$ is the general time varying load vector.

TANK-LIQUID FINITE ELEMENT COMPUTATIONAL MODEL

In current research the finite element model of a cylindrical water tank, designed and constructed in Armenia is selected. The tank is made up of 5mm steel plate. The internal diameter of the tank is D=11.4m. The height of the tank till the roof slope is H=10.3m. The roof of the tank is also made up of 5mm steel plate, supported by long and short support girders. The slope of the roof is selected to be approximately 20%. For analysis purposes, three strategies of a) empty, b) 50% full and c) 100% full is taken into account. Figure 2 shows the 3D finite element model of the tank, containing filling strategies. In finite element model of the anchored tank, four-node quadrilateral shell elements are used for modelling of surrounding wall, bottom and the roof. Two-node linear elements are used to model the roof rafters. For modelling of the liquid, eight-node brick acoustic elements are used. The acoustic finite elements use linear wave theory and consider the dilatational motion of the liquid. The interaction between liquid and tank is considered using definition “Surface tied normal contact constraint” between the interfaces of liquid and tank.

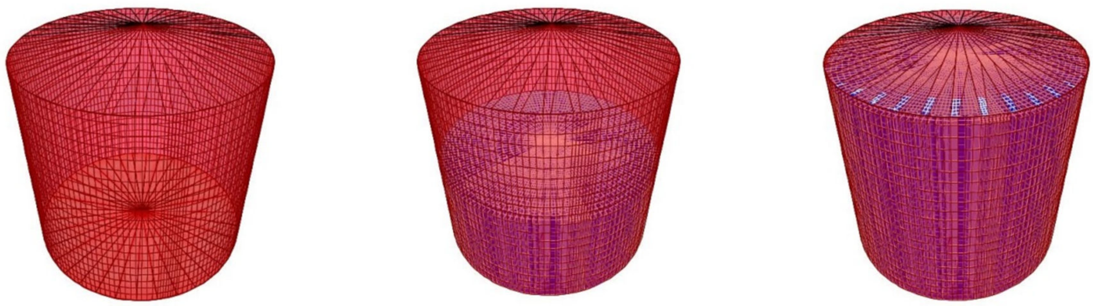

(a) (b) (c)

Fig. 2 - Proposed finite element models: (a) Empty, (b) 50% Full, (c) 100% Full

This constraint is formulated based on a master-slave contact method, in which normal force is transmitted using tied normal contact between both surfaces through the simulation, letting the sloshing modes in liquid to be formed. The freeboard is taken into account 30 cm.

TIME HISTORY ANALYSES

In order to perform the time history analyses, 5 pair of accelerograms of earthquakes recorded on each soil type, according to Armenian SNIP II-2.06 code, were selected. Then each pair was scaled to spectral acceleration level of S_a=0.35g. Selected records are of the earthquakes listed in Table 1.

Table 1 - Characteristics of used Earthquake Records

Event	Year	Mag.	Mechanism
Superstition Hills	1987	6.54	Strike-Slip
Chi-Chi-Taiwan	1999	7.62	Reverse-Oblique
Irpinia-Italy	1980	6.9	Normal
Tabas-Iran	1978	7.35	Reverse
Denali-Alaska	2002	7.9	Strike-Slip
Loma Prieta	1989	6.93	Reverse-Oblique
Kocaeli-Turkey	1999	7.51	Strike-Slip
Northridge	1994	6.69	Reverse
San Fernando	1971	6.61	Reverse
Landers	1992	7.28	Strike-Slip
Hector Mine	1999	7.13	Strike-Slip
Cape Mendocino	1992	7.01	Reverse
Westmorland	1981	5.9	Strike-Slip
Imperial Valley	1979	6.53	Strike-Slip

The scale factor for an accelerogram computed based on the larger PGA of its two horizontal components. Then both horizontal components are multiplied by the computed scale factor. Then the scaled records were applied to the computational models separately due to the soil type and spectral acceleration for which the selected model was analysed and designed. For Time history analyses, the “Direct Integration” technique was used. Time history analyses for all models were completed using Newmark - β method using γ = 0.5 & β = 0.25. Due to structural characteristics, the damping ratio for linear analyses was determined equal to 0.05 for the first two modes of vibration.

NUMERICAL RESULTS

The final results of the Fluid-Structure Interaction analysis of the tank-reservoir system are indicated in Table 2.

Table 2 Fluid-Structure analysis results, Base shear force versus percent of Filling

Soil Category	Acceleration No.	Filling %	Base Shear Force (Ton)
		0	666.6
	1	50	975.5
		100	1757.8
		0	373.8
	2	50	561.5
		100	1020.7

		0	437.8
SI (Rock)	3	50	612.2
		100	856.0
		0	503.9
	4	50	767.0
		100	1044.9
		0	657.6
	5	50	860.9
		100	1593.7
		0	356.9
	1	50	492.3
		100	822.8
		0	284.5
	2	50	499.1
		100	746.9
		0	455.2
SII (Dense Soil)	3	50	636.1
		100	1053.9
		0	391.8
	4	50	553.9
		100	891.2
		0	315.9
	5	50	460.1
		100	676.2
		0	385.8
	1	50	618.1
		100	939.3
		0	477.6
	2	50	670.7
		100	936.7
		0	469.4
SIII (Loose Soil)	3	50	817.4
		100	1062.7
		0	390.9
	4	50	662.8
		100	1111.3
		0	361.9
	5	50	555.3
		100	807.2
		0	467.2
	1	50	655.2
		100	919.5
		0	463.0
	2	50	680.4
		100	1004.1

SIV (Very Loose Soil)	3	0 50 100	369.6 609.5 787.1
	4	0 50 100	500.1 842.0 1077.0
	5	0 50 100	379.0 727.6 888.2

For the results of the analyses to be apparent, they are converted into diagrams of base shear force versus percent of filling. The mentioned diagrams are shown in Figure 3.

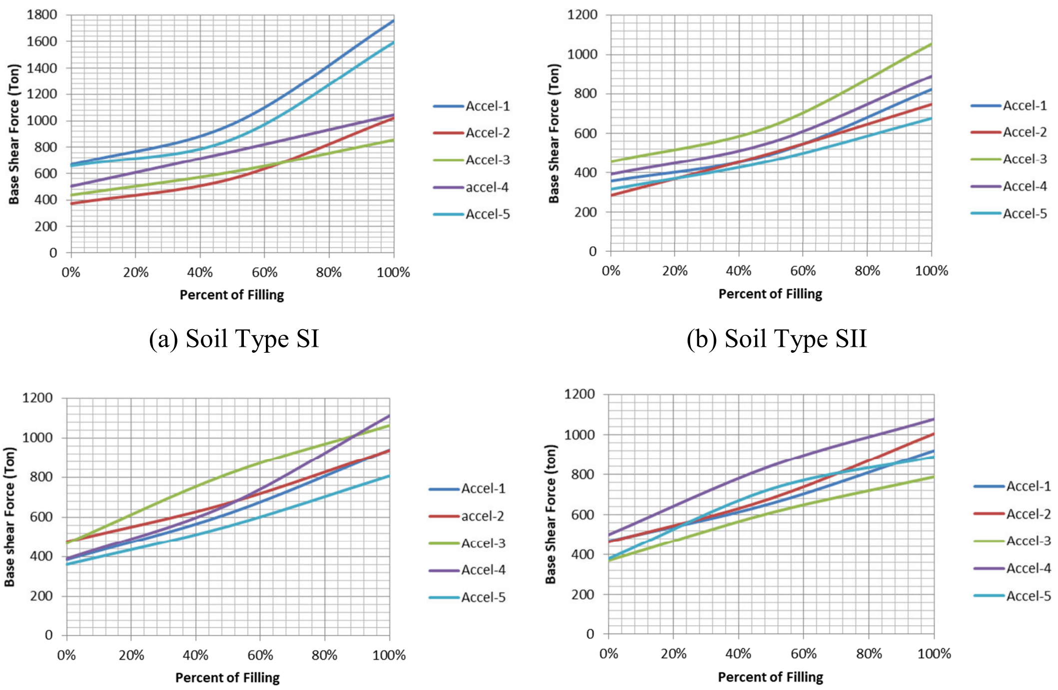

(a) Soil Type SI (b) Soil Type SII

(c) Soil Type SIII (d) Soil Type SIV

Fig. 3 - Diagrams of Base Shear Forces versus Percent of Filling according to soil categories

CONCLUSION

The computational results of the finite element analysis of the whole Fluid-Structure system for several filling strategies illustrate that by degrading the soil category, the amplification of the base shear force due to tank filling percent converts to be linear for loose soils rather than parabolic in case of dense soils. As could be observed in diagrams of Figure 3, when the tank starts to get filled for more than 50% of it's full capacity, base shear forces start to increase nonlinearly, mainly in case of soil type SI and partially for soil type SII. When degrading the soil category, this event starts to get reduced. According to the diagrams in Figure 3, the most significant effects of this kind could be observed in case of Soil type SI. In case of this soil category, the maximum amplification of base shear force is almost accessible for most of earthquake records, when the tank is started to get filled more than 50% of it's full capacity. According to this fact, in case of soil type SI, the maximum effect of sloshing mode of liquid caused by convetive mass of water inside is predictible. In case of soil type SII~SIV, one could observe the small effect of soil degradation on the sloshing mode of vibration of the liquid inside the tank. On the other hand, the impulsive mass of the liquid has almost the same effect on the Fluid-Structure system behavior in case of all soil categories up to 100% of filling strategy. Soil type SI seems to be an exception, for which the impulsive mass of the liquid is working up to 50% of filling capacity, after which the convective mass is activated. It could be concluded that degrading the soil category from SI to SIV, lessens the seismic response of the circular water tanks with medium H/D ratio by reducing the effect of sloshing mode of the liquid caused by convective mass, while the effect of the impulsive mass is remained almost the same for all soil categories.

ACKNOWLEDGMENTS

The authors gratefully acknowledge the funding by ESS-Consulting Engineering Company, for completing current research.

REFERENCES

[1] Chopra A.K., 2012, Dynamics of Structures:Theory and applications to Earthquake Engineering (4th ed.), Prentice Hall,Englewood Cliffs.

[2] Dogangun A., Ayvaz, Y. and Durmus, A., 1997, Earthquake Analysis of Water Tanks, 4th International Conference on Civil Engineering, Vol 1, Sharif University of Technology, pp. 400-409.

[3] Housner, G.W., 1963, Dynamic Behavior of Water Tanks, Bulletin of the Seismological Society of America, Vol. 53, pp. 381-387.

[4] Shaaban, S.H. and Nash, W.A. (1976), “Finite element analysis of a seismically excited cylindrical storage tanks, ground supported and partially filled with liquid”, Report NSF/RA-760261, University of Massachusetts.

[5] SNIP II-6.02, “Armenian Code of Practice for Seismic Resistant Design of Buildings”, 2006.

[6] Wilson, E.L. and Khalvati, M., 1983, Finite element for the dynamic analysis of fluid-solid system. Int. J. No.19.